Frustration in the Kondo lattice model: Local versus extended singlet phases

B. H. Bernhard,[1,*] B. Coqblin,[2] and C. Lacroix[3]

[1]*Departamento de Física, Universidade do Estado de Santa Catarina, Joinville, Santa Catarina, Brazil*

[2]*Laboratoire de Physique des Solides, CNRS–Université Paris-Sud, Orsay, France*

[3]*Institut Néel, CNRS–Université Joseph Fourier, Grenoble, France*

(Received 26 February 2011; revised manuscript received 3 May 2011; published 30 June 2011)

We present a theoretical study of the frustrated Kondo lattice model on a Shastry-Sutherland-type lattice. Using a mean-field decoupling on both the Kondo and intersite exchange interactions, we study three different phases, an antiferromagnetic (AF) phase without Kondo effect, a Kondo (K) phase without magnetic order, and finally a valence bond solid (VBS) phase without magnetic order and Kondo effect. A phase diagram is obtained giving the stability region of the three phases, as a function of the Kondo parameter J_K and the frustration ratio J/J' of the two exchange interactions on the Shastry-Sutherland lattice. This phase diagram can account for the change under pressure from a nonmagnetic Kondo phase to an AF phase and to a completely different nonmagnetic VBS phase occurring in some ytterbium compounds such as Yb_2Pd_2Sn.

DOI: 10.1103/PhysRevB.83.214427 PACS number(s): 75.20.Hr, 75.10.Kt, 75.10.Jm

I. INTRODUCTION

Competition between Kondo effect and magnetism is often described by the Kondo lattice Hamiltonian, and this competition leads to the well-known Doniach diagram:[1] if the Kondo interaction J_K is large compared to the intersite Ruderman-Kittel-Kasuya-Yosida (RKKY) exchange J_{ij}, the ground state is a nonmagnetic Kondo state, while for small J_K, RKKY interactions favor an antiferromagnetic state. This diagram gives a good description of many heavy-fermion compounds,[2] in which the quantum critical point (QCP), which separates the two ground states, can be reached either by applying pressure or by doping.[3] However, in some cases the magnetic interactions are strongly frustrated, either due to long-range competing interactions or due to the geometry of the lattice, and magnetic ordering is strongly suppressed. There are several examples of heavy-fermion compounds in which frustration of magnetic interactions plays an important role (for a review, see Ref. 4).

The search for a global phase diagram, extending the Doniach phase diagram to include frustration effects, is an active issue. In Refs. 5 and 6, a qualitative phase diagram has been proposed, as a function of the Kondo interaction and frustration. This phase diagram suggests that, depending on the relative values of these parameters, the ground state can be magnetic or not, and two different nonmagnetic states were proposed. However, in both papers, only qualitative discussions were presented. In the present paper, we show explicitly a model where Kondo effect and frustration are present, and we characterize the different phases by different order parameters. The obtained phase diagram is in agreement with the proposals made in Refs. 5 and 6. Moreover, our calculation shows that mean-field decoupling is a good starting point for describing this phase diagram.

Here we study the Kondo lattice problem in the Shastry-Sutherland geometry,[7] illustrated in Fig. 1. A realization of this lattice with localized spins was first reported for $SrCu_2(BO_3)_2$,[8] and it has been mainly explored theoretically within the pure Heisenberg model.[9–11] Recently, several heavy-fermion cerium and ytterbium compounds exhibiting this geometry have been experimentally studied[12–16] and for some of them the phase diagram under pressure or alloying has been obtained. In fact, applied pressure can have opposite effects in Kondo cerium and ytterbium compounds. In particular, for Yb compounds, pressure often makes the local Kondo parameter J_K decrease[17,18] and can give rise to a transition from a Kondo phase to a magnetic one in the usual Doniach picture. In the presence of frustration, pressure can induce a transition to a nonmagnetic valence bond or to a spin liquid phase, if magnetic order is destabilized by frustration. Both the Kondo and valence bond phases are nonmagnetic, but they have completely different properties. We propose in this paper that this phase diagram can account for the pressure dependence of ytterbium compounds such as Yb_2Pd_2Sn[14,15] and YbAgGe,[13,19,20] as we will see in more detail in the discussion, although this last compound has a different crystallographic structure.

For localized quantum spins in the Shastry-Sutherland lattice, strong frustration leads to a nonmagnetic ground state which can be constructed as a superposition of dimer singlet states, while for weak frustration an antiferromagnetic state with $\mathbf{q} = (\pi,\pi)$ is stable. In the case of a Kondo lattice, the absence of magnetism in the Shastry-Sutherland lattice can also be due to frustration, but the Kondo effect alone can lead to a nonmagnetic ground state as well. It is thus interesting to study the competition between both effects, the Kondo interaction leading to the formation of local singlets, while the frustrated intersite exchange leads to valence bond singlets.

In the next section, we introduce a model Hamiltonian for the Shastry-Sutherland lattice describing a system of local spins $\mathbf{S}_i$ and a conduction band coupled through a local Kondo interaction J_K at every site. We adopt a mean-field decoupling which leads to an effective noninteracting fermionic Hamiltonian, consisting of hybridized bands. In Sec. III, we describe the phase diagram of the model. In the last section, we discuss the results in connection with the experimental phase diagram of some Ce and Yb compounds.

II. MODEL HAMILTONIAN AND APPROXIMATION

The Hamiltonian of the Kondo lattice can be written as

$$\mathcal{H} = \mathcal{H}_H + \mathcal{H}_t + \mathcal{H}_K, \tag{1}$$

 ©2011 American Physical Society

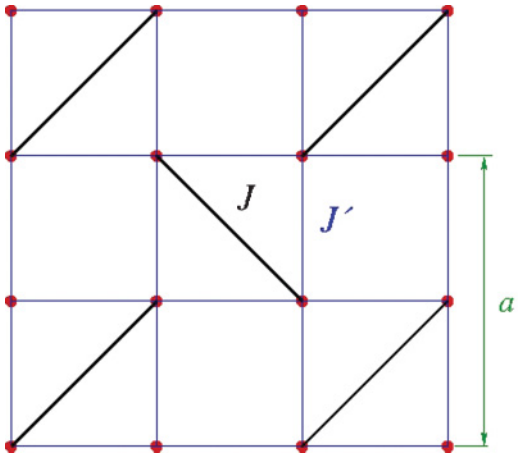

FIG. 1. (Color online) The Shastry-Sutherland lattice. In compounds like Yb_2Pd_2Sn (Ref. 14), the distance between the sites forming the orthogonal dimers (linked by the thick diagonal lines) is reduced and they become nearest neighbors. The thin lines connect the next-nearest neighbors, drawing a distorted square lattice. Along the thick and thin lines the exchange interactions between localized spins are respectively equal to J and J'. The lattice can be regarded as a square lattice with a basis consisting of four atoms with a lattice parameter a.

where

$$\mathcal{H}_H = \frac{1}{2}\sum_{ij} J_{ij}\,\mathbf{S}_i\cdot\mathbf{S}_j, \tag{2}$$

$$\mathcal{H}_t = -\sum_{ij\sigma} t_{ij}\,c^\dagger_{i\sigma}c_{j\sigma}, \tag{3}$$

$$\mathcal{H}_K = J_K\sum_i \mathbf{S}_i\cdot\mathbf{s}_i. \tag{4}$$

The first term $\mathcal{H}_H$ describes a Heisenberg lattice of localized spins $\mathbf{S}_i$ interacting via exchange interactions J_{ij}. The second term $\mathcal{H}_t$ describes a tight-binding conduction electron band, and $\mathcal{H}_K$ is the local Kondo coupling between localized spins $\mathbf{S}_i$ and conduction electron spins $\mathbf{s}_i$ ($J_K > 0$).

On the Shastry-Sutherland lattice, the exchange parameters J_{ij} take two different values J and J', as indicated in Fig. 1, when sites i and j are connected by a diagonal or a nondiagonal bond, respectively. In the following both J and J' are considered as positive. Frustration can be varied by changing the ratio J/J'.[7,9–11] For strong frustration, $J \gg J'$, the ground state consists of singlet dimers formed along the diagonal bonds, while for weak frustration, $J \ll J'$, the ground state is the two-sublattice antiferromagnetic (AF) state on the square lattice. The critical value of J/J' which separates these two ground states is of the order of 1.5.[10]

Here we add to this model conduction electrons interacting with the localized spins through a Kondo exchange coupling J_K. The conduction band is described in tight-binding approximation by hopping integrals t_{ij} which can assume the two values t and t' along diagonal and nondiagonal bonds. In the following, all parameters like J and t will refer to diagonal bonds, while J' and t' will refer to the square lattice bonds.

In fact, in Kondo lattice systems, the exchange interactions between localized spins are induced by the local Kondo coupling J_K: this is the usual RKKY exchange. The magnitude of J and J' is then proportional to $\rho(E_F)J_K^2$, where $\rho(E_F)$ is the density of states of the conduction band at the Fermi level and their signs depend on the Fermi wave vector k_F. Thus they can be ferro- or antiferromagnetic. However, to explore the complete phase diagram, we consider here J_K, J, and J' as independent parameters, and we restrict our attention to the frustrated case where both J and J' are positive.

We introduce the fermionic representation for the localized spin $S = 1/2$. The components of the spin operators are written in terms of creation and annihilation operators $f^\dagger_{i\sigma}$ and $f_{i\sigma}$:

$$S^z_i = \tfrac{1}{2}\left(n^f_{i\uparrow} - n^f_{i\downarrow}\right), \tag{5}$$

$$S^\sigma_i = S^x_i + i z_\sigma S^y_i = f^\dagger_{i\sigma} f_{i\bar{\sigma}}, \tag{6}$$

where $n^f_{i\sigma} = f^\dagger_{i\sigma} f_{i\sigma}$ is the f-electron number operator, and $z_\uparrow = +1$, $z_\downarrow = -1$. Similar expressions can be used for the conduction electron spins $\mathbf{s}_i$ in terms of operators $c^\dagger_{i\sigma}$ and $c_{j\sigma}$.

Substitution of these expressions into Eqs. (2) and (4) generates products of four fermionic operators, which are decoupled in a mean-field approximation.[2,21] Here we study three different types of ground state: (i) a magnetically ordered (AF) state; this is the expected ground state for $J \ll J'$ (no frustration) and small T_K, where T_K is the Kondo energy scale; (ii) a correlated Kondo (K) phase; this phase should be the ground state for large enough T_K; and (iii) a valence bond solid (VBS) state, where spins on the dimers are strongly coupled along the diagonals; this should be the ground state when $J \gg J'$ and $J \gg T_K$. For this purpose we introduce the following averages:

$$\lambda_{i\sigma} = \langle f^\dagger_{i\sigma} c_{i\sigma}\rangle, \tag{7}$$

$$\tilde{\gamma}^\sigma_{ij} = \langle f^\dagger_{j\sigma} f_{i\sigma}\rangle, \tag{8}$$

and

$$\gamma^\sigma_{ij} = \langle c^\dagger_{j\sigma} c_{i\sigma}\rangle. \tag{9}$$

The mean-field parameter $\lambda_{i\sigma}$ describes the local c-f correlations due to the Kondo effect, while $\tilde{\gamma}^\sigma_{ij}$ describe the intersite spin correlations in absence of long-range order.[2,21]

After dropping constant terms, we obtain an effective fermionic Hamiltonian describing hybridized, uncorrelated bands:

$$\mathcal{H}' = \mathcal{H}_t + \mathcal{H}_{\tilde{t}} + \mathcal{H}_{\tilde{V}} + \mathcal{H}_f + \mathcal{H}_h, \tag{10}$$

where

$$\mathcal{H}_{\tilde{t}} = -\sum_{ij\sigma} \tilde{t}^\sigma_{ij}\, f^\dagger_{i\sigma} f_{j\sigma}, \tag{11}$$

$$\mathcal{H}_{\tilde{V}} = -\sum_{i\sigma} \tilde{V}_{i\sigma}(f^\dagger_{i\sigma} c_{i\sigma} + c^\dagger_{i\sigma} f_{i\sigma}), \tag{12}$$

$$\mathcal{H}_f = E_f \sum_{i\sigma} f^\dagger_{i\sigma} f_{i\sigma}, \tag{13}$$

$$\mathcal{H}_h = \sum_{i\sigma} z_\sigma\left(h^f_i + \tilde{h}_i\right) n^f_{i\sigma} + \sum_{i\sigma} z_\sigma h^c_i n^c_{i\sigma}. \tag{14}$$

The effective parameters depend on the self-consistent mean-field parameters:

$$\tilde{t}_{ij}^{\sigma} = \tfrac{1}{2} J_{ij}\left(\tilde{\gamma}_{ij}^{\bar{\sigma}} + \tfrac{1}{2}\tilde{\gamma}_{ij}^{\sigma}\right), \tag{15}$$

$$\tilde{V}_{i\sigma} = \tfrac{1}{2} J_K\left(\lambda_{i\bar{\sigma}} + \tfrac{1}{2}\lambda_{i\sigma}\right), \tag{16}$$

$$h_i^f = \tfrac{1}{2} J_K \langle s_i^z \rangle, \tag{17}$$

$$h_i^c = \tfrac{1}{2} J_K \langle S_i^z \rangle, \tag{18}$$

and

$$\tilde{h}_i = \frac{1}{2}\sum_j J_{ij}\langle S_j^z \rangle. \tag{19}$$

The local molecular fields h_i^c and h_i^f imply a magnetic coupling between local and itinerant moments.

The energy E_f is a Lagrange multiplier introduced in Eq. (13) in order to impose the constraint on the f -electron number

$$\sum_{\sigma} \langle n_{i\sigma}^f \rangle = n_f = 1. \tag{20}$$

As usual in mean-field approximation, the constraint is fixed for the average f-electron number. In the same way, the chemical potential μ is fixed from the constraint

$$\sum_{\sigma} \langle n_{i\sigma}^c \rangle = n_c, \tag{21}$$

where n_c is the conduction electron concentration.

We apply the Green's function method to the effective hamiltonian $\mathcal{H}'$ in order to evaluate the averages of interest. For the Shastry-Sutherland lattice, it is convenient to introduce an index α to label the four atoms of the basis located at a given site i of the underlying square lattice. The standard fermionic Green's functions involving operators $c_{i\alpha\sigma}$ and $f_{i\alpha\sigma}$ are then obtained easily and allow calculation of the band structure of the system. In general, there are 16 bands per unit cell (eight for each spin direction), since the unit cell consists of four sites, with c and f electrons on each site, and the parameters are spin dependent. Details of the calculation are given in the Appendix.

The solution described in the Appendix is valid for all phases, including the antiferromagnetic phase and the nonmagnetic phase as the limit of vanishing staggered magnetizations $\langle S^z \rangle$ and $\langle s^z \rangle$. We presume translational invariance over the square basis, with a site-independent $\lambda_{i\sigma}$ on each sublattice, and the averages $\tilde{\gamma}_{ij}^{\sigma}$ and γ_{ij}^{σ} assuming the same values $\tilde{\gamma}_{\sigma}$,γ_{σ} along all diagonal bonds, and $\tilde{\gamma}'_{\sigma}$,γ'_{σ} along all square lattice bonds. The effective hopping parameters $\tilde{t}_{ij}^{\sigma}$ introduced in Eq. (15) are equal to $\tilde{t}$ or $\tilde{t}'$ corresponding to $J_{ij} = J$ or J', and $\tilde{\gamma}_{ij}^{\sigma} = \tilde{\gamma}^{\sigma}$ or $\tilde{\gamma}'^{\sigma}$. The effective hybridization $\tilde{V}_{i\sigma}$ in Eq. (16) is also site independent on each sublattice. Assuming AF order, Eq. (19) yields $\tilde{h} = \frac{1}{2}(J - 4J')\langle S^z \rangle$. In this case, we also note that *a priori* $\tilde{\gamma}'^{\sigma} = \tilde{\gamma}'^{\bar{\sigma}}$, but $\tilde{\gamma}^{\sigma} \neq \tilde{\gamma}^{\bar{\sigma}}$ and $\lambda_{i\sigma} \neq \lambda_{i\bar{\sigma}}$.

In terms of the effective parameters, the internal energy per site for the complete Hamiltonian $\mathcal{H}$ in Eq. (1) can be expressed as

$$E = -\frac{1}{2}\sum_{\sigma} \tilde{t}_{\sigma}\tilde{\gamma}^{\sigma} - 4\tilde{t}'\tilde{\gamma}' - t\sum_{\sigma}\gamma_{\sigma} - 8t'\gamma' - \sum_{\sigma}\tilde{V}_{\sigma}\lambda^{\sigma} + \tilde{h}\langle S^z \rangle + J_K\langle S^z \rangle\langle s^z \rangle. \tag{22}$$

This expression can be used to find the minimum energy state for a given set of parameters (J, J', t, t', J_K, and the number of conduction electrons n_c). In the next section we will study some peculiar solutions, corresponding to the three phases described in the Introduction.

III. RESULTS

The physical properties of the model are determined by the competition among the multiple phases described by the self-consistent parameters λ_{σ}, $\tilde{\gamma}_{\sigma}$, $\tilde{\gamma}'$, $\langle S^z \rangle$, and $\langle s^z \rangle$. We restrict our attention here to phases with unit cell similar to the crystallographic unit cell, and we have studied the following phases:

(i) the AF phase in the absence of the Kondo effect, which corresponds to the solution with $\lambda_{\sigma}, \tilde{\gamma}_{\sigma}, \tilde{\gamma}' = 0$ and $\langle S^z \rangle, \langle s^z \rangle \neq 0$;

(ii) the K phase without magnetic order, which corresponds to the solution $\lambda_{\sigma}, \tilde{\gamma}, \tilde{\gamma}' \neq 0$ and $\langle S^z \rangle, \langle s^z \rangle = 0$;

(iii) the VBS frustrated phase without magnetic order and Kondo effect, which corresponds to the solution with $\lambda_{\sigma}, \langle S^z \rangle, \langle s^z \rangle, \tilde{\gamma}' = 0$, and $\tilde{\gamma}_{\sigma} \neq 0$. This solution can be considered a particular case of the K solution, without any Kondo effect, but we have studied it separately, since it is expected to be stable in the pure Shastry-Sutherland model with large frustration.

In Ref. 6 the possibility of d_{xy} superconducting instability in both the VBS and K phases was also proposed. Superconductivity could also be studied in the present model, by introducing pairing order parameters with various symmetries. More complex phases could also be studied, as for example a mixed antiferromagnetic-Kondo phase where the Kondo effect is present in the antiferromagnetic phase.

A. Zero-temperature phase diagram

By comparing the respective energies at $T = 0$, we obtain the phase diagram illustrated in Fig. 2. The results correspond to a particular choice of parameters $J' = 0.5t'$, $t = 0.1t'$, and a band filling $n_c = 0.9$. The parameter J_K/t' measures the strength of the Kondo effect, and J/J' measures the degree of frustration. The value of t/t' does not play an important role: it modifies the band structure but as long as the Fermi level falls within a band, the results are not qualitatively changed. To avoid peculiar physics in the half-filled case (for example, the half-filled Kondo lattice can be insulating), we take in the following the band filling n_c equal to 0.9. Of course, the precise position of the transition lines between the three phases depends on the conduction band parameters: t/t' and n_c.

For large J_K/t', the K phase dominates due to the large Kondo effect, and for large J/J', strong frustration leads to the VBS solution. As expected, the AF phase is stable in the region where both J_K/t' and J/J' are small, i.e., when the Kondo effect and frustration are weak. We observe that a minimum

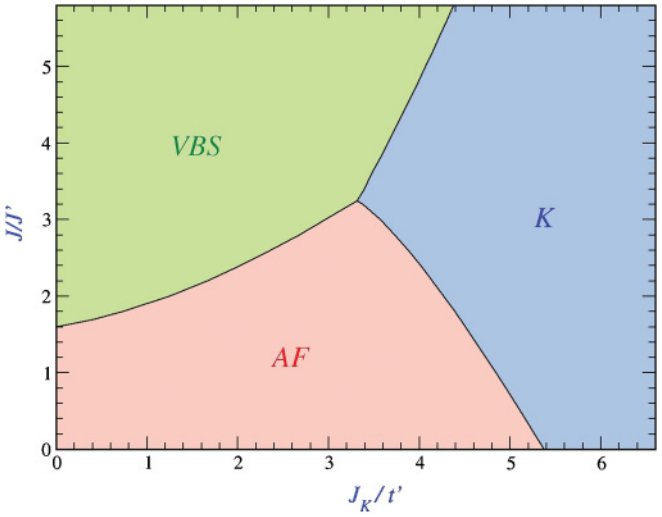

FIG. 2. (Color online) Phase diagram of the Shastry-Sutherland Kondo lattice model for $J' = 0.5t'$, $t = 0.1t'$, and $n_c = 0.9$. For the definition of the three phases (VBS, AF, and K) see the text. In the mean-field approximation, all transitions are discontinuous.

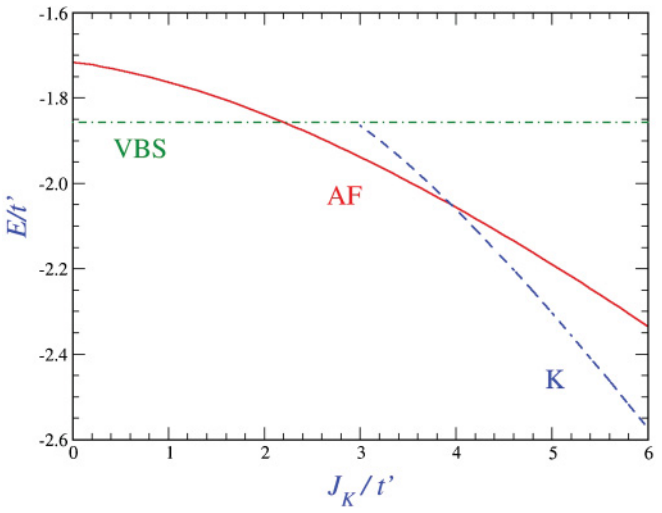

FIG. 3. (Color online) Internal energies of the three solutions K (dashed), AF (solid), and VBS (dot-dashed) as a function of J_K/t' for $J' = 0.5t'$, $t = 0.1t'$, $n_c = 0.9$, and $J = 2.5J'$.

value of J_K is required for the solution $\lambda \neq 0$, as in the nonfrustrated Doniach diagram. At $J_K = 0$, where the model reduces to the pure Heisenberg Hamiltonian decoupled from the conduction electrons, the transition between the AF phase and the VBS phase occurs at $J/J' \approx 1.60$ (or $J'/J \approx 0.625$). This value is quite close to the results reported from other approaches developed for the $S = 1/2$ Shastry-Sutherland model.[10,11]

Figure 3 shows the ground-state energies of the three solutions listed above for $J/J' = 2.5$. When J_K/t' decreases, the ground state changes from the Kondo state to the AF state and then to the VBS state. There is a finite region of J_K where the AF phase is stable, between two different nonmagnetic phases. The existence of these two different nonmagnetic phases, stable in different regions of parameter space, is the main result of our model. These nonmagnetic phases, the low-J_K phase and the high-J_K phase, are completely different: the low J_K one is a VBS, in which the localized spins are coupled into singlet dimers, while, in the high-J_K Kondo phase, magnetism disappears because of the local screening of the localized spins due to the Kondo interaction. For small J/J', frustration is weak and, with increasing J_K, the system goes from the AF to the K phase as in a nonfrustrated Kondo lattice. For larger J/J', AF is destabilized and the ground state is a VBS as long as the Kondo effect remains small. For large enough J_K, of course, the ground state is again a Kondo phase.

Figure 3 also shows that the transitions between the different phases are first order in this approach: the mean-field parameters do not vanish at the transition, and the transitions are discontinuous.

To understand more precisely the transition between VBS and K states, we have studied the strongly frustrated case $J/J' = 4$ for which AF is never stable. As illustrated in Fig. 4, the transition between VBS and K states is discontinuous. For $J_K/t' < 3.47$, the VBS state is the ground state, and $\tilde{\gamma}$ is the only nonvanishing mean-field parameter. For $J_K/t' > 4.28$, the Kondo state is the ground state, with large λ and small $\tilde{\gamma}$ and $\tilde{\gamma}'$. In the intermediate region, three solutions are found: the VBS one, and two Kondo solutions, with large and small λ respectively. Comparison of the energies of the three solutions (inset of Fig. 4) shows that the K solution with small λ is never stable, and there is a discontinuous first-order transition between the K and VBS states at $J_K/t' \approx 3.66$.

It should be pointed out that the present approximation gives reliable results for the VBS phase: in this phase, the parameter $\tilde{\gamma}$ is equal to -0.5 at $T = 0$, while $\tilde{\gamma}'$ vanishes. This leads to a magnetic energy per site equal to $-3J/8$, which is exactly

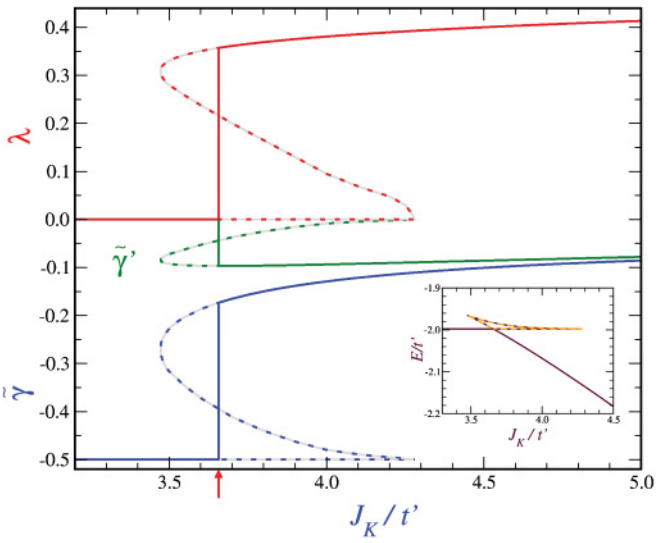

FIG. 4. (Color online) Mean-field parameters as a function of J_K/t' for $J' = 0.5t'$, $t = 0.1t'$, $n_c = 0.9$, and $J = 4J'$. Continuous lines correspond to the stable solution, and dotted lines correspond to unstable or metastable solutions. The arrow in the horizontal axis indicates the location of the first-order phase transition. The energies of the three solutions are illustrated in the inset.

the value expected in the VBS state, when all diagonal bonds are forming singlets.

It was proposed in Ref. 6 that the transition between the Kondo and VBS phases might be a quantum critical transition while, in the present approach, it is a first-order transition. To go further in the study of this transition would require going beyond the mean-field approximation.

B. Evolution at finite temperature

We have also studied the evolution of the three phases with increasing temperature. Of course, since the model is a two-dimensional one, no phase transition is expected at finite temperature, while the mean field always gives phase transitions: if fluctuations around the mean field are considered, critical temperatures become crossover temperatures below which the different types of correlation (AF, Kondo, or intradimer correlations) are growing.

Figure 5 shows the self-consistent averages $\langle S^z\rangle$, $\langle s^z\rangle$, $\tilde{\gamma}$, and λ as a function of temperature for $J' = 0.5t'$, $t = 0.1t'$, $n_c = 0.9$, and $J = 2.5J'$ for different values of J_K/t' corresponding to the three phases AF, K, and VBS. The magnetization curves drop to zero at the Néel temperature T_N [Fig. 5(a)]. The Kondo temperature T_K is taken as the temperature at which the parameter λ goes to zero [Fig. 5(c)]. In the Kondo phase, the parameters $\tilde{\gamma}$ and $\tilde{\gamma}'$ are nonzero, but they remain small: they describe the magnetic correlations in the Kondo phase as in Ref. 2. We can also introduce a characteristic temperature T_{VBS} at which the parameter $\tilde{\gamma}$ vanishes in the VBS phase [Fig. 5(b)].

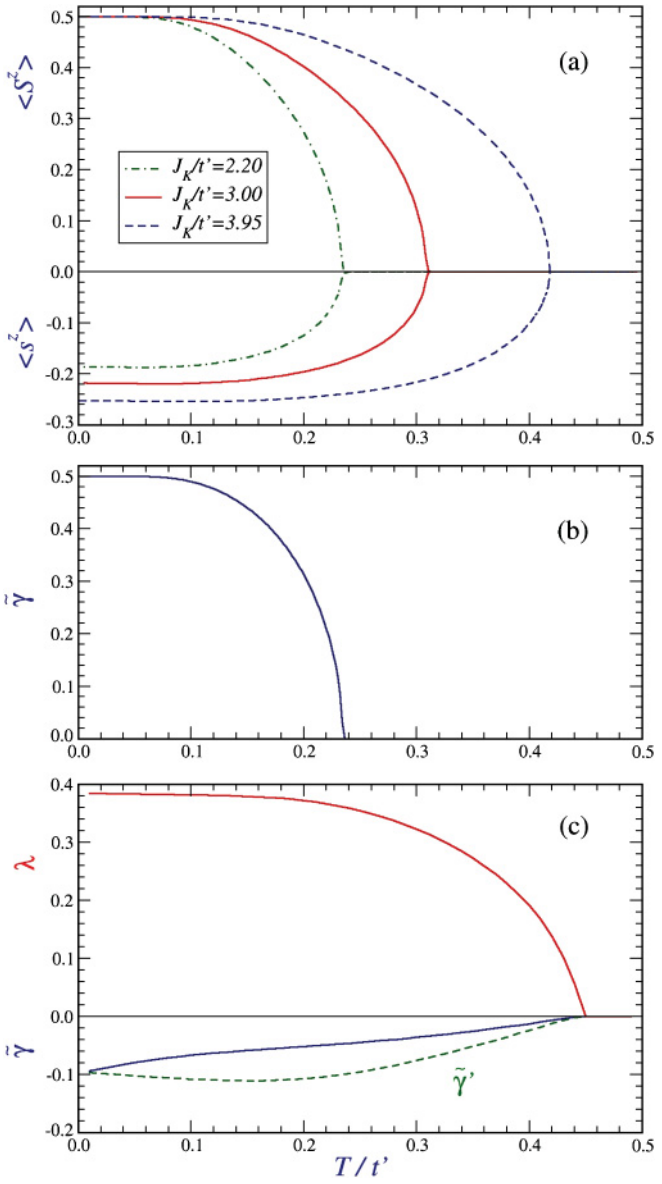

FIG. 5. (Color online) Mean-field parameters as a function of temperature for $J' = 0.5t'$, $t = 0.1t'$, $n_c = 0.9$, and $J = 2.5J'$: (a) magnetizations $\langle S^z\rangle$ and $\langle s^z\rangle$ in the AF phase for different values of J_K/t'; (b) average $\tilde{\gamma}$ in the VBS phase for $J_K/t' = 2.20$; (c) averages $\tilde{\lambda}$, $\tilde{\gamma}$, and $\tilde{\gamma}'$ in the K phase for $J_K/t' = 3.95$.

IV. DISCUSSION

It is well known that the increase of pressure gives an increase of J_K/t' in cerium compounds and a decrease in ytterbium compounds.[2,17,18] This effect has been observed in many cerium and ytterbium compounds, leading to a transition between Kondo and magnetic ground states which is well understood within the Doniach diagram. By including frustration, we have obtained here a different phase diagram presented in Fig. 2 with an additional nonmagnetic phase, where the absence of magnetism is due to frustration of intersite exchange and not to the Kondo effect.

In the present case, the theoretical behavior presented in Fig. 2 can account for the pressure dependence of some ytterbium compounds and we will first discuss the very clear examples provided by Yb_2Pd_2Sn (Refs. 14,15) and YbAgGe.[13] The crystallographic structure of Yb_2Pd_2Sn has the same topology as the Shastry-Sutherland lattice and it is clearly a nonmagnetic Kondo compound with a large electronic specific heat coefficient $\gamma = 560$ mJ/mol K^2 at low temperatures and normal pressure. It becomes antiferromagnetic above 1 GPa. The Néel temperature increases rapidly up to a maximum of 1.2 K at 2.5 GPa and then it decreases to 4 GPa, where it undergoes a transition to a nonmagnetic state. We propose that Yb_2Pd_2Sn goes from a Kondo state to an AF order and finally to a nonmagnetic frustrated state, in good agreement with Fig. 2 for decreasing J_K/t' with an intermediate value of J/J' ($J/J' \approx 2.5$). A similar behavior has also been observed by applying chemical pressure in the doped compound $Yb_2Pd_2In_{1-x}Sn_x$, where there are successively, with increasing x, a nonmagnetic phase, then an antiferromagnetically ordered phase for x roughly between 0.4 and 0.9, and finally another nonmagnetic phase.[14] The first nonmagnetic phase is a Kondo one and the second could be reminiscent of the VBS phase. In fact, this high-pressure phase has not been much studied, but, if it is a VBS phase, it should be quite different from the low-temperature Kondo phase: the specific heat coefficient γ should be significantly smaller, since in the VBS phase the effective c-f hybridization vanishes. The magnetic properties of the two phases should also be different: the Kondo phase has no spin gap, while the VBS phase has a spin gap.

The compound YbAgGe has a different crystallographic structure, similar to the kagome geometry,[13,19,20] which is

also strongly frustrated. It undergoes two successive magnetic transitions at 0.8 and 0.65 K. When pressure is applied, these two temperatures merge at 0.5 GPa into one $T_N = 0.8$ K, which remains nearly constant up to 1.5 GPa; then it increases rapidly to about 1.7 K at 3.2 GPa, reaches a maximum of 5.4 K at a pressure of 6.8 GPa, and drops less rapidly to 2.2 K at 13.8 GPa. The extrapolated zero value of T_N corresponds roughly to a pressure of 16 GPa. Such an experimental behavior can also be well accounted for by our model, although this compound is a kagome lattice: at normal pressure, YbAgGe is a heavy-fermion antiferromagnet very close to the AF-Kondo transition; when pressure increases, J_K/t' decreases and the Néel temperature increases rapidly as expected in the classical Doniach diagram; then, there is the transition from AF to the nonmagnetic frustrated state, which causes a decrease of T_N, and finally the disappearance of the magnetic order. Of course, the phase diagram of Fig. 2 was obtained for a Shastry-Sutherland lattice, but the same competition between local Kondo and intersite frustrated exchange interactions is present in the kagome geometry: the pure kagome lattice, with isotropic nearest-neighbor interactions J is fully frustrated and has a spin liquid (SL) ground state at $T = 0$ (for a review on the kagome lattice, see Ref. 23), but if additional interaction, such as next-nearest-neighbor coupling J', is introduced, magnetic ordering occurs above some critical value of J'/J. In this case, the phase diagram would include a SL phase at small J'/J and small J_K (instead of the VBS phase), a Kondo phase at large J_K, and a magnetically ordered phase (AF) at large J'/J and small J_K. We propose that with increasing pressure this compound goes from K to AF and then to SL phases.

There are presently many other cerium and ytterbium compounds in which frustration effects are present, such as, for instance, Yb_2Pt_2Pb,[12] CePdAl,[22] Ce_2Pd_2Sn,[24] Ce_2Pt_2Pb, or Ce_2Ge_2Mg,[16] but in fact their magnetic behavior cannot be interpreted simply in our model. For example, CePdAl has a mixed magnetic structure with coexistence of magnetic and nonmagnetic sites, which is stabilized by frustration.[4] In Ce_2Pd_2Sn, the results suggest that the diagonal exchange J is ferromagnetic.[24,25] Yb_2Pt_2Pb is magnetically ordered, and it was proposed in Ref. 12 that this compound is close to the critical point. The large specific heat coefficient observed in this system (311 mJ/Yb mol K^2) might be an indication of a Kondo effect. Very recently, two additional interesting cerium compounds of this family have been studied: Ce_2Pt_2Pb and Ce_2Ge_2Mg.[16]

In summary, we have obtained the ground-state phase diagram for heavy-fermion compounds with the Shastry-Sutherland lattice geometry. We have shown that, in addition to the Kondo and antiferromagnetic phases, a VBS phase can be stable if frustration is large enough. The results are consistent with recent observations on the compound Yb_2Pd_2Sn, but further experiments are necessary to confirm our interpretation. The same kind of phase diagram should be obtained in other geometries, like the kagome one, as found in compounds with crystal structure similar to YbAgGe. More generally, when frustration is considered in the Kondo lattice model, a more complex phase diagram is obtained which contains an additional type of phase and possible transitions between two different nonmagnetic ground states. This type of transition implies a change in electronic structure and Fermi surface topology, since in the VBS phase, electrons states are decoupled from the localized spins. Such transition is sometimes classified as a Lifshitz transition in the literature.[26,27] In the present description it is first order. Further studies would be necessary to get a better description of this transition. Moreover, further experimental data on cerium and ytterbium compounds are needed, in order to obtain a well-defined VBS phase under pressure or in alloys and to study the nature of the transitions between the different phases.

ACKNOWLEDGMENT

B.H.B. wishes to acknowledge the support of the Brazilian agency Fundação de Amparo à Pesquisa do Estado de Santa Catarina (FAPESC).

APPENDIX: GREEN'S FUNTIONS METHOD

The Green's functions are defined in the usual way as

$$G^{ff,\sigma}_{i\alpha,j\beta}(\omega) = \langle\langle\, f_{i\alpha\sigma}; f^{\dagger}_{j\beta\sigma}\rangle\rangle, \tag{A1}$$

and similar expressions for $G^{cc,\sigma}_{i\alpha,j\beta}(\omega)$ and $G^{fc,\sigma}_{i\alpha,j\beta}(\omega)$.

The equations of motion corresponding to the effective Hamiltonian $\mathcal{H}'$ in Eq. (10) read

$$\left(\omega - z_\sigma h^c_i\right)G^{cc,\sigma}_{i\alpha,j\beta} = \delta_{ij}\delta_{\alpha\beta} - \tilde{V}^{\sigma}_{i\alpha}G^{fc,\sigma}_{i\alpha,j\beta} - \sum_{k\delta} t_{i\alpha,k\delta}G^{cc,\sigma}_{k\delta,j\beta}, \tag{A2}$$

$$\left(\omega - E_f - z_\sigma h^f_i - z_\sigma \tilde{h}_i\right)G^{fc,\sigma}_{i\alpha,j\beta} = -\tilde{V}^{\sigma}_{i\alpha}G^{cc,\sigma}_{i\alpha,j\beta} - \sum_{k\delta}\tilde{t}^{\sigma}_{i\alpha,k\delta}G^{fc,\sigma}_{k\delta,j\beta}, \tag{A3}$$

$$\left(\omega - E_f - z_\sigma h^f_i - z_\sigma \tilde{h}_i\right)G^{ff,\sigma}_{i\alpha,j\beta} = \delta_{ij}\delta_{\alpha\beta} - \tilde{V}^{\sigma}_{i\alpha}G^{cf,\sigma}_{i\alpha,j\beta} - \sum_{k\delta}\tilde{t}^{\sigma}_{i\alpha,k\delta}G^{ff,\sigma}_{k\delta,j\beta}, \tag{A4}$$

$$(\omega - z_\sigma h^c_i)G^{cf,\sigma}_{i\alpha,j\beta} = -\tilde{V}^{\sigma}_{i\alpha}G^{ff,\sigma}_{i\alpha,j\beta} - \sum_{k\delta} t_{i\alpha,k\delta}G^{cf,\sigma}_{k\delta,j\beta}. \tag{A5}$$

The system of equations is solved by spatial Fourier transformation

$$G^{ff,\sigma}_{i\alpha,j\beta}(\omega) = \frac{1}{N}\sum_{\mathbf{q}} G^{ff,\sigma}_{\alpha\beta}(\mathbf{q},\omega)e^{i\mathbf{q}\cdot(\mathbf{R}^{\alpha}_i - \mathbf{R}^{\beta}_j)}, \tag{A6}$$

where $\mathbf{R}^{\alpha}_i$ is the position of the αth atom at the ith site of the lattice.

Equations (A2)–(A5) can then be expressed in matrix form as

$$\mathbb{M}_\sigma(\mathbf{q},\omega)\mathbb{G}^{cc}_\sigma(\mathbf{q},\omega) = \mathbb{I} - \widetilde{\mathbb{V}}_\sigma \mathbb{G}^{fc}_\sigma(\mathbf{q},\omega), \tag{A7}$$

$$\widetilde{\mathbb{M}}_\sigma(\mathbf{q},\omega)\mathbb{G}^{fc}_\sigma(\mathbf{q},\omega) = -\widetilde{\mathbb{V}}_\sigma \mathbb{G}^{cc}_\sigma(\mathbf{q},\omega), \tag{A8}$$

$$\widetilde{\mathbb{M}}_\sigma(\mathbf{q},\omega)\mathbb{G}^{ff}_\sigma(\mathbf{q},\omega) = \mathbb{I} - \widetilde{\mathbb{V}}_\sigma \mathbb{G}^{cf}_\sigma(\mathbf{q},\omega), \tag{A9}$$

$$\mathbb{M}_\sigma(\mathbf{q},\omega)\mathbb{G}^{cf}_\sigma(\mathbf{q},\omega) = -\widetilde{\mathbb{V}}_\sigma \mathbb{G}^{ff}_\sigma(\mathbf{q},\omega), \tag{A10}$$

where

$$\mathbb{M}_\sigma(\mathbf{q},\omega) = \begin{pmatrix} \omega - z_\sigma h^c & 2t'\cos(x/2) & te^{i(x-y)/2} & 2t'\cos(y/2) \\ 2t'\cos(x/2) & \omega + z_\sigma h^c & 2t'\cos(y/2) & te^{i(x+y)/2} \\ te^{-i(x-y)/2} & 2t'\cos(y/2) & \omega - z_\sigma h^c & 2t'\cos(x/2) \\ 2t'\cos(y/2) & te^{-i(x+y)/2} & 2t'\cos(x/2) & \omega + z_\sigma h^c \end{pmatrix}, \tag{A11}$$

$$\widetilde{\mathbb{M}}_\sigma(\mathbf{q},\omega) = \begin{pmatrix} \omega - E_f - z_\sigma(h^f + \tilde{h}) & 2\tilde{t}'\cos(x/2) & \tilde{t}_\sigma e^{i(x-y)/2} & 2\tilde{t}'\cos(y/2) \\ 2\tilde{t}'\cos(x/2) & \omega - E_f + z_\sigma(h^f + \tilde{h}) & 2\tilde{t}'\cos(y/2) & \tilde{t}_{\bar\sigma} e^{i(x+y)/2} \\ \tilde{t}_\sigma e^{-i(x-y)/2} & 2\tilde{t}'\cos(y/2) & \omega - E_f - z_\sigma(h^f + \tilde{h}) & 2\tilde{t}'\cos(x/2) \\ 2\tilde{t}'\cos(y/2) & \tilde{t}_{\bar\sigma} e^{-i(x+y)/2} & 2\tilde{t}'\cos(x/2) & \omega - E_f + z_\sigma(h^f + \tilde{h}) \end{pmatrix}, \tag{A12}$$

with $x = q_x a$ and $y = q_y a$,

$$\widetilde{\mathbb{V}}_\sigma = \begin{pmatrix} \tilde{V}_\sigma & 0 & 0 & 0 \\ 0 & \tilde{V}_{\bar\sigma} & 0 & 0 \\ 0 & 0 & \tilde{V}_\sigma & 0 \\ 0 & 0 & 0 & \tilde{V}_{\bar\sigma} \end{pmatrix} \tag{A13}$$

is the hybridization matrix, and $\mathbb{I}$ is the 4×4 identity matrix.

The closed algebraic solution is obtained by an inverse Fourier transformation. Finally, the averages are calculated from the corresponding elements of the matrix Green's functions.

*dfi2bhb@joinville.udesc.br

[1] S. Doniach, Physica B **91**, 231 (1977).

[2] J. R. Iglesias, C. Lacroix, and B. Coqblin, Phys. Rev. B **56**, 11820 (1997).

[3] P. Coleman, in *Handbook of Magnetism and Advanced Magnetic Materials*, Vol. 1, edited by Helmut Kronmuller and Stuart Parkin (John Wiley and Sons, London, 2010), Vol. 1.

[4] C. Lacroix, J. Phys. Soc. Jpn. **79**, 011008 (2010).

[5] Q. Si, Physica B **378–380**, 23 (2006).

[6] P. Coleman and A. H. Nevidomskyy, J. Low Temp. Phys. **161**, 182 (2010).

[7] B. S. Shastry and B. Sutherland, Physica B **108**, 1069 (1981).

[8] H. Kageyama, K. Yoshimura, R. Stern, N. V. Mushnikov, K. Onizuka, M. Kato, K. Kosuge, C. P. Slichter, T. Goto, and Y. Ueda, Phys. Rev. Lett. **82**, 3168 (1999).

[9] S. Miyahara and K. Ueda, Phys. Rev. Lett. **82**, 3701 (1999).

[10] S. Miyahara and K. Ueda, J. Phys.: Condens. Matter **15**, R327 (2003).

[11] M. Albrecht and F. Mila, Europhys. Lett. **34**, 145 (1996).

[12] M. S. Kim, M. C. Bennett, and M. C. Aronson, Phys. Rev. B **77**, 144425 (2008).

[13] K. Sengupta, M. K. Forthaus, H. Kubo, K. Katoh, K. Umeo, T. Takabatake, and M. M. Abd-Elmeguid, Phys. Rev. B **81**, 125129 (2010).

[14] E. Bauer, H. Michor, T. Muramatsu, T. Kanemasa, T. Kagayama, K. Shimizu, Y. Aoki, H. Sato, and M. Giovannini, J. Optoelectron. Adv. Mater. **10**, 1633 (2008).

[15] F. Kikuchi, K. Hara, E. Matsuoka, H. Onodera, S. Nakamura, T. Nojima, K. Katoh, and A. Ochiai, J. Phys. Soc. Jpn. **78**, 083708 (2009).

[16] M. S. Kim and M. C. Aronson, J. Phys.: Condens. Matter **23**, 164204 (2011).

[17] J. Plessel, M. M. Abd-Elmeguid, J. P. Sanchez, G. Knebel, C. Geibel, O. Trovarelli, and F. Steglich, Phys. Rev. B **67**, 180403 (2003).

[18] O. Trovarelli, C. Geibel, S. Mederle, C. Langhammer, F. M. Grosche, P. Gegenwart, M. Lang, G. Sparn, and F. Steglich, Phys. Rev. Lett. **85**, 626 (2000).

[19] H. Kubo, K. Umeo, K. Katoh, A. Ochiai, and T. Takabatake, J. Phys. Soc. Jpn. **77**, 023704 (2008).

[20] H. Kubo, K. Umeo, K. Katoh, A. Ochiai, and T. Takabatake, J. Phys. Soc. Jpn. **79**, 064715 (2010).

[21] P. Coleman and N. Andrei, J. Phys.: Condens. Matter **1**, 4057 (1989).

[22] A. Oyamada, S. Maegawa, M. Nishiyama, H. Kitazawa, and Y. Isikawa, Phys. Rev. B **77**, 064432 (2008).

[23] P. Mendels and A. Wills, in *Introduction to Frustrated Magnetism*, edited by C. Lacroix, P. Mendels, and F. Mila, Springer Series in Solid State Sciences (Springer-Verlag, Berlin, 2011), Vol. 164.

[24] J. G. Sereni, M. Gomez Berisso, G. Schmerber, and J. P. Kappler, Phys. Rev. B **81**, 184429 (2010).

[25] J. G. Sereni, M. Gomez Berisso, A. Braghta, G. Schmerber, and J. P. Kappler, Phys. Rev. B **80**, 024428 (2009).

[26] A. Hackl and M. Vojta, Phys. Rev. B **77**, 134439 (2008).

[27] Y. Yamaji, T. Misawa, and M. Imada, J. Phys. Soc. Jpn. **75**, 094719 (2006).